

Spectroscopic study of self-organized quantum dot like structures in Ga–In–P superlattices on (311) GaAs

Sandip Ghosh^{a)} and B. M. Arora

Solid State Electronics Group, Tata Institute of Fundamental Research, Homi Bhabha Road, Mumbai 400 005, India

Seong-Jin Kim, Joo-Hyong Noh, and Hajime Asahi

The Institute of Scientific and Industrial Research, Osaka University, 8-1, Mihogaoka, Ibaraki, Osaka- 567, Japan

Received 28 July 1998; accepted for publication 30 November 1998)

We report temperature dependent photoluminescence, contactless electroreflectance and photoluminescence excitation study of $(\text{GaP})_2(\text{InP})_{2.5}$ strained short period superlattices sandwiched between $\text{Ga}_x\text{In}_{1-x}\text{P}$ alloy layers grown on GaAs (311)A substrates. Transmission electron microscope pictures of these samples reveal the presence of self-organized In rich globular structures with Ga rich surroundings in the superlattice planes. The variation of the peak position of the photoluminescence band with decreasing temperature has an anomalous dip. We show that this is not due to an anomalous change in the band gap with temperature but is due to the interplay between two luminescence pathways associated with two phases, one which has the original $(\text{GaP})_2(\text{InP})_{2.5}$ superlattice and the other being the self-organized composition modulated In rich regions within the superlattice layers. We also present spectroscopic results which indicate quantum dot like nature of the self-organized In rich structures in these samples. © 1999 American Institute of Physics. [S0021-8979(99)03905-5]

I. INTRODUCTION

In recent years it has been a challenge to grow high quality and high density of semiconductor quantum dots (QDs) for making semiconductor lasers as they are expected to have significantly improved characteristics such as higher optical gain, lower threshold current density, greater thermal stability, etc. One route being explored for fabricating such structures is that of self-organized growth.¹ Improved performance of lasers based on InAs QDs, formed via strain induced Stranski–Krastanow growth mode, has already been demonstrated.² However InAs QD lasers emit only in the infrared while it is desirable to have QD based lasers over wider spectral range. Fafard *et al.*³ using InAlAs alloy (larger band gap than InAs) based QDs have demonstrated lasers which emit red light (707 nm). Another self-organized growth mechanism namely strain induced lateral composition modulation (SILCM) has been shown to give rise to alternate regions of Ga rich and In rich lamellae in the (001) plane oriented along $[\bar{1}10]$ direction during the growth of $(\text{GaP})_m(\text{InP})_n$ short period superlattice (SPS) on GaAs (001) substrates.⁴ Evidence for this composition modulation was obtained from transmission electron microscope (TEM) pictures, energy dispersive x-ray analysis (EDX) and polarization dependent spectroscopic measurements.^{5,6} It has been proposed that the process leading to this composition modulation is initiated by strongly anisotropic diffusion of the group III atoms on the GaAs surface and thereafter is sustained by strain induced nucleation of excess adatoms.⁷ Use

of these self-organized structures as building blocks to fabricate semiconductor quantum wire lasers has been demonstrated.⁸

Thereafter Kim *et al.*⁹ showed that the SILCM process can give rise to QD-like structures when the $(\text{GaP})_m(\text{InP})_n$ SPS are grown on GaAs (N11) substrates as evidenced from TEM pictures and scanning tunneling microscopy (STM) studies.¹⁰ It was also reported that some of these samples did not show the expected regular increase in the photoluminescence (PL) peak energy position with decreasing temperature.⁹ There have been several other reports of anomalous temperature dependence of PL peak positions in Ga–In–P based systems some of which have been attributed to ordered alloy formation.^{11,12} Wohlerl *et al.*¹³ have reported anomalously weak temperature dependence of the PL peak positions in samples where SILCM modified layers form the building blocks, to explain which they proposed a hypothesis involving multiaxial strains which counterbalance the normal temperature dependence of the band gap. However in the case of broad PL features, interplay between different luminescence mechanisms with different temperature dependence can give rise to misleading results. Since PL is often dominated by transitions involving defects/impurities, the information obtained from it about the band structure is less satisfactory. A modulation spectroscopy experiment such as contactless electroreflectance (CER) does not suffer from these drawbacks and can also identify higher lying critical points in the band structure¹⁴ and therefore is better suited to examine this issue.

In this paper we present the results of PL (including its dependence on the excitation intensity), CER and photoluminescence excitation (PLE) measurements on samples which

^{a)}Present address: Physics Dept., University of Surrey, Guildford GU2 5XH, United Kingdom; Electronic mail: s.ghosh@surrey.ac.uk

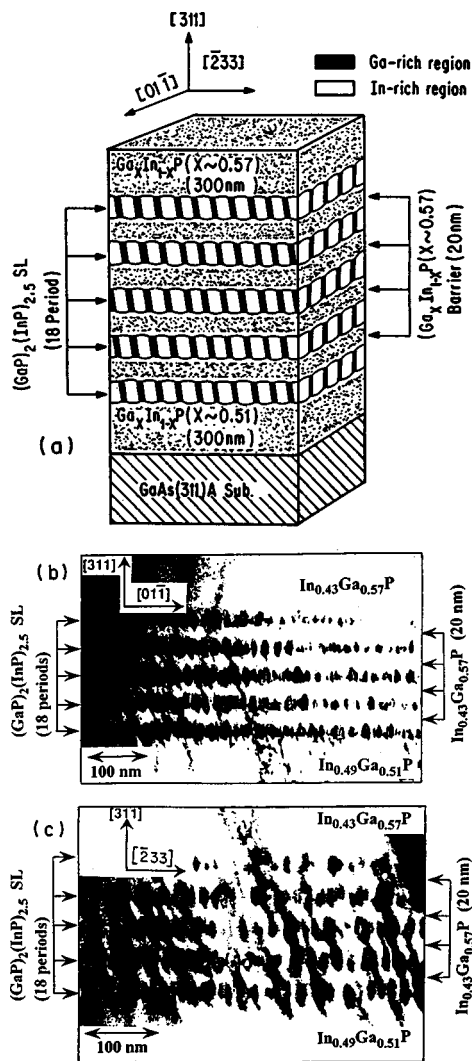


FIG. 1. (a) Schematic of the sample structure. (b),(c) TEM pictures of the sample (side view, $[233]$ and $[01\bar{1}]$ faces, respectively) showing the alternating bright In rich and dark Ga rich regions within the SPS layers.

have SILCM induced QD-like structures and whose PL peak position shows an anomalous dip. Comparing the results of temperature dependent CER and PL spectroscopy, we identify the origins of the features in the PL spectrum, determine the PL quenching pathway and provide an explanation for the anomalous temperature dependence of the PL peak positions. A simple preliminary calculation has also been made to determine the optical transition energies in these Ga–In–P alloy based QDs whose results are compared with experimental observations.

II. EXPERIMENT

The samples used in this study were grown by gas source molecular beam epitaxy. Several samples were grown with different GaP/InP layer thickness on differently oriented GaAs substrates.^{9,10} From among them, the present study concentrates on the sample which shows maximum anomaly in the temperature dependence of its PL peak position. The sample structure is shown schematically in Fig. 1(a). It consists of five layers of 18 period $(\text{GaP})_2(\text{InP})_{2.5}$ SPS sand-

wiched between 200 Å layers of $\text{Ga}_x\text{In}_{1-x}\text{P}$ alloy. This was grown on a Si doped GaAs (311)A substrate with an undoped GaAs buffer layer, followed by another 3000 Å $\text{Ga}_x\text{In}_{1-x}\text{P}$ alloy buffer layer and was finally capped by a 3000 Å $\text{Ga}_x\text{In}_{1-x}\text{P}$ alloy layer at the top. The intended nominal value of x in the alloy layers was 0.51, however spectroscopic and high resolution x-ray diffraction measurements suggest that the value of $x \approx 0.57$ both in the cap alloy layer as well as the alloy layers in between the SPS layers. Figures 1(b) and 1(c) show the TEM pictures of the sample (side view) which reveal alternate bright and dark patches within the SPS layers. EDX studies on samples grown on (001) substrates⁸ showed that the bright regions in the SPS layers are In rich while the darker regions are Ga rich. The Ga/In composition contrast is typically found to be $\approx 40\%/60\%$ in this system. STM studies on the SPS planes of the sample in Fig. 1 show that the Ga/In rich regions form globular structures with a distribution in diameters.¹⁰ The distribution (average for $[01\bar{1}]$ and $[\bar{2}33]$ directions) can be approximated by a Gaussian with a mean diameter of ≈ 210 Å and a full width at half maximum of ≈ 50 Å. Since InP has a smaller band gap than GaP, from the point of view of electronic band structure, the In rich globules within the SPS layers represent potential troughs for electrons and holes surrounded on four sides by the Ga rich regions which act as barriers. The $\text{Ga}_{0.57}\text{In}_{0.43}\text{P}$ alloy layers in between the SPS layers act as barriers in the vertical direction so as to confine the carriers in the In rich regions of the SL from all directions making them into QDs. The details of the growth and structural characterization have been reported earlier.^{9,10}

In the PL experiments, the excitation source was an Ar^+ ion laser (488 nm). The luminescence was detected using a photomultiplier tube (S20 type response) after it was dispersed by a 1/8 m monochromator with 1 nm band pass. The sample was cooled using a closed cycle helium refrigerator. In the PLE experiments, light from a 150 W quartz–tungsten–halogen (QTH) lamp, dispersed using a 1/8 m monochromator with ≈ 3.5 nm bandpass was used as the excitation source. In the CER^{15,16} measurements, the sample was placed between two electrodes in a capacitor like arrangement with the top electrode kept ≈ 0.3 mm from the sample surface. A 1 kV (rms) sinusoidal voltage was applied on the top transparent electrode to modulate the sample's surface electric field. The probe beam was obtained by dispersing light from a 150 W QTH lamp using a 1/8 m monochromator with ≈ 4 nm bandpass and detected using a silicon photodetector. In all cases phase sensitive detection of the signal was made using a lock-in amplifier.

III. RESULTS AND DISCUSSION

A. Temperature dependence

Figures 2(a) and 2(b) show the PL spectra at two different spots A and B on the sample at various temperatures. Apart from the large widths of the PL spectra, it is quite clear from the large shifts of the main 8 K PL feature's peak position between spots A and B that the sample is inhomogeneous. The magnified high energy end of the 8 K PL spectra show two more features which have been labeled P1 and

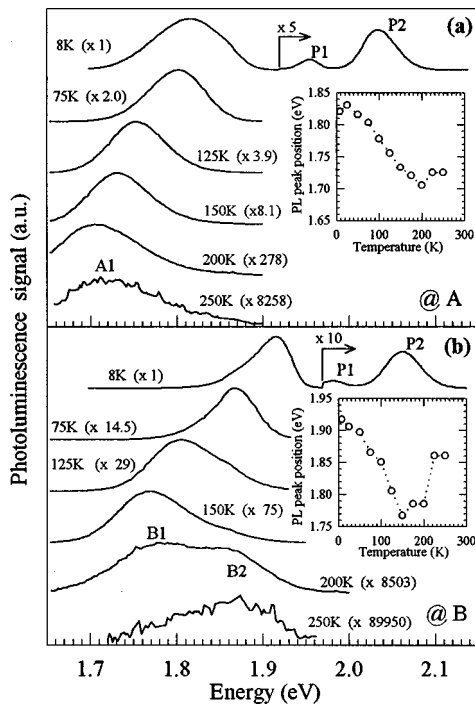


FIG. 2. PL spectra at two different spots A (a) and B (b) on the sample at various temperatures. The 200 K spectrum at B indicates the presence of two features which are labeled B1 and B2. The insets show the temperature dependence of the peak position of the dominant PL features at the two spots. The dotted lines are a guide to the eye.

P2. The peak positions of these features show relatively much smaller shifts between spot A and B. The spectra at A and B represent the two extreme PL peak positions in this sample. We observed that the PL peak position tends to vary monotonically along [011] while remaining practically unchanged along the [233] direction. The insets in Figs. 2(a) and 2(b) show the variation of the dominant PL feature's peak position at spots A and B, respectively, as a function of temperature. It is evident that while the temperature dependence of the peak position of the dominant PL feature at B shows a large anomalous dip, that for A is closer to normal. Significantly, the 200 K PL spectrum at spot B gives clear indication that there are two features which have been labeled as B1 and B2. The single main feature at A has been labeled A1.

Fitting a single Gaussian to feature A1 and a sum of two Gaussians to the feature at B we estimated the integrated intensity of the main PL features at the two spots as a function of temperature. The symbols in Fig. 3 represent a logarithmic plot of the integrated PL intensity as a function of inverse temperature for the PL features A1 (circles), B1 (triangles) and B2 (squares). The lines represent a fit to the data using the following equation:¹⁷

$$I(T)_{PL} = I_0 / [1 + \gamma \exp(-Q/k_B T)] \quad (1)$$

where $I(T)_{PL}$ is the integrated PL intensity at a given temperature T , Q is the activation energy for PL quenching, I_0 is the intensity at the lowest temperature and γ has been interpreted as the ratio of the radiative lifetime to the minimum nonradiative lifetime for carrier decay. The value of Q is found to be 243 ± 10 meV for A1; while it is 244 ± 10 meV

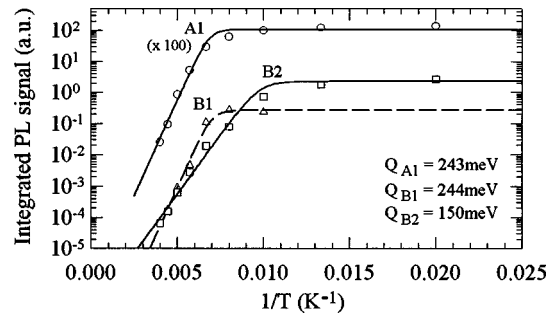


FIG. 3. The temperature dependence of the integrated PL intensity for features A1 (circle), B1 (triangle) and B2 (square). The lines are fits to Eq. (1). The plots for feature A1 have been shifted up ($\times 100$) for clarity.

and 150 ± 10 meV for B1 and B2, respectively. From Figs. 2(b) and 3 it is clear that the anomaly in the temperature dependence of the PL peak position arises because the feature B1, which has a different energy position as compared to B2, dominates the spectrum in the temperature range 200–125 K while B2 dominates in the rest of the temperature range.

To further confirm that the PL peak position anomaly is not due to an anomalous temperature dependence of the band gaps we performed CER measurements on this sample. Figure 4 shows typical CER spectra of the sample at spots A and B at 8 K. In both these spectra we can identify three major transitions shown as C1, C2 and C3. A feature due to the GaAs substrate also arises at lower energies but because it is unimportant in the present context, it has not been shown here. The transition energies of these features were estimated by separately fitting to them the following line shape function:

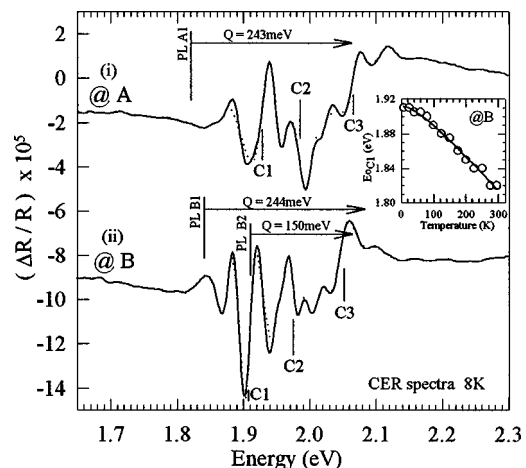


FIG. 4. Contactless electroreflectance spectrum of the sample at the two different spots A and B. The plots are vertically shifted for clarity. The three major transitions seen in both the spectra have been labeled C1, C2 and C3. The dotted lines represent the line shape function in Eq. (2) fitted separately to these features. The inset (circles) shows the temperature dependence of the energy position of transition C1 while the line represents a fit to the Varshni equation (3).

$$\Delta R/R = \sum_{j=1}^n \operatorname{Re}[a_j \exp(i\theta_j)/(E - E_{0j} + i\Gamma_j)^m],$$

$$i = \sqrt{-1},$$
(2)

where E_{0j} , Γ_j , θ_j and a_j are the transition energy, broadening parameter, phase factor and amplitude, respectively, associated with the j th transition. In the above equation the value of m used was 3, which mimics the case of a first derivative Gaussian broadened line shape function¹⁴ applicable in the case of inhomogeneous broadening of the critical point energies in quantum confined systems. The fitted curves are shown by the dotted lines in Fig. 4. The inset in Fig. 4 (circles) shows the temperature dependence of the transition energy of the lowest energy CER feature C1 which clearly shows no anomalous dip. It is also evident that the transition energy of lowest energy feature (C1) in the CER spectra at the two spots A and B does not have the large shift that is observed in the case of the dominant features in the 8 K PL spectra at these two spots.

Before discussing the origins of the PL features A1, B1 and B2 in detail, we shall briefly comment on the origins of the dominant CER features C1, C2, C3 and the PL features P1, P2. From the composition dependence of the band gap of $\text{Ga}_x\text{In}_{1-x}\text{P}$ alloys, the feature C3 around 2.06 eV is identified as the signature of the transition at the band gap of the $\text{Ga}_{0.57}\text{In}_{0.43}\text{P}$ random alloy which forms the cap layer and the layers in between the SPS layers. Based on the peak energy position, the PL feature P2 can also be identified as being associated with this alloy. The feature C2 and the associated PL feature P1 arise from the buffer $\text{Ga}_{0.51}\text{In}_{0.49}\text{P}$ alloy layer at the bottom. Comparing the feature C1 with photoreflectance spectroscopy measurements and calculations of Armelles *et al.*¹⁸ on $(\text{GaP})_m(\text{InP})_n$ SPS grown on GaAs (001) substrates we identify it as being associated with the $(\text{GaP})_2(\text{InP})_{2.5}$ SPS layers in our sample. The difference (≈ 50 meV) in the transition energy values for the SPS structure in our sample and those of Armelles *et al.* arises most likely due to the m/n ratio being different and also because of the different strains that the SPS layer is subjected to on a (311) substrate as compared to a (001) substrate.

The origins of the features A1, B1 and B2 can be understood as follows. Within the SPS layer there exist two phases, one which is the original SPS structure and the other the SILCM modified phase having In rich globular structures with Ga rich surroundings. The PL features A1 and B1 arise from the In rich regions of the latter phase and have QD-like characteristics to be discussed subsequently. The PL feature B2 whose peak position is coincident with the CER feature C1, arises from the unmodified SPS phase. The difference between the spots A and B is the extent of SILCM induced modification. Because the modification is more at A (high QD density), nearly all the photogenerated carriers are collected by the QDs while at B where the modification is less (low QD density), the unmodified SPS phase also contributes to the PL signal. The larger extent of the modification of the SPS layers at A as compared to B is also indicated by the broader CER feature C1 at A as compared to B. The rela-

tively small difference in the PL peak positions of A1 and B1 (see the 150 K PL spectra at the two spots) is most likely due to the difference in the size and composition distribution (In content) of the QDs at A and B. However we do not see any signature of the QDs in the CER spectra. This is not surprising since their low density (as compared to bulk) and inhomogeneous broadening due to dot size and composition distribution make detection of the QDs in the CER spectra very difficult. In fact in the only definitive identification of self-organized QDs by CER reported so far (InAs QDs on GaAs),¹⁹ the signal strength was $\Delta R/R \approx 2 \times 10^{-6}$, that too with narrower dot size distribution and uniform composition.

We see that the activation energy values for thermal quenching of PL (Q) for A1 and B1 are nearly identical and differ considerably from that for B2. This can be understood as follows. In the case of quantum confined systems such as quantum wells it is found that the activation energy for PL quenching is equal to the difference between the PL emission energy and the barrier band gap,²⁰ indicating that the PL quenching involves simultaneous thermal emission of the electron and the hole, constituting an exciton, into energy levels corresponding to the adjacent barriers from where they can recombine both radiatively as well as nonradiatively. At the barrier energy the latter process is normally dominant since carriers are no longer confined to a small region and therefore encounter more defects which increase the probability of nonradiative recombination considerably. In our case, for the carriers confined in the SPS phase, the effective barriers are expected to be the $\text{Ga}_{0.57}\text{In}_{0.43}\text{P}$ alloy layers in between the SPS layers. This explains the 150 ± 10 meV value of Q for B2, since as shown in the Fig. 4 plot (ii), at an energy 150 ± 10 meV higher than the peak position of the PL feature B2 lies the CER feature C3 associated with the $\text{Ga}_{0.57}\text{In}_{0.43}\text{P}$ alloy layers. The carriers in the QDs are expected to see two kinds of barriers: $\text{Ga}_{0.57}\text{In}_{0.43}\text{P}$ alloy layers in the vertical direction (direction of growth) and SILCM modified Ga rich surroundings in the (311) plane. In Fig. 4 plots (i) and (ii), it is again seen that at an energy $\approx 243 \pm 10$ meV (equal to the activation energy for PL quenching for A1 and B1) higher than the peak positions of PL features A1 and B1 lies in the CER feature C3 indicating that the $\text{Ga}_{0.57}\text{In}_{0.43}\text{P}$ alloy layers also act as effective barriers for the QDs. This is in accordance with the fact that the $\text{Ga}_{0.57}\text{In}_{0.43}\text{P}$ alloy barrier layers have lower Ga content than the Ga rich parts of the SILCM modified phase ($\geq 60\%$) and therefore the former represents a lower barrier height for the carriers in the QDs. We also see that the effective barrier height for the carriers in the QDs as compared to those in the SPS phase is larger, which explains why the quenching of the QD luminescence starts at higher temperature than the quenching of the SPS luminescence. This suggests the possibility of higher room temperature QD luminescence efficiency if the band gap of the barrier layers can be increased by incorporating a small amount of Al in them.

The above discussion also suggests that the estimation of temperature dependence of critical point energies from PL peak shifts can be misleading in the case of QD related emission with large widths arising from inhomogeneities in dot size and composition (another source of error will be dis-

cussed in Sec. III B). The width implies different effective barrier heights and therefore different activation energies; those for the dots emitting at longer wavelengths is larger than those emitting at shorter wavelengths. As the temperature is raised the luminescence from the QDs emitting at longer wavelengths are therefore less likely to decay and cause a more rapid shift of the peak to longer wavelengths than expected from band gap narrowing alone. We note here that the above mentioned mechanism of quenching of QD related PL signals (which modifies the temperature dependence of the PL peak position for an ensemble of QDs with large size distribution) has previously been reported for self assembled InGaAs/GaAs and InAlAs/AlGaAs QDs.²¹ In the present case, the presence of the CER features at similar energies above the PL peak position as the activation energies for PL quenching gives further proof of this mechanism of PL quenching.

The temperature dependence of the CER transition energies follows the temperature dependence of the critical point energies accurately and are not affected by the above mentioned source of error. Unfortunately the CER signature for the QDs could not be seen in our experiments most likely because the inhomogeneous broadening due to QD size and composition variation makes the CER signals of the QDs too weak to be detectable. The lowest energy CER feature C1 seen by us is associated with the SPS phase. Fitting the temperature dependence of transition energy of feature C1 (continuous line in the inset of Fig. 4) to the empirical Varshni relation:²²

$$E_g(T) = E_{g0} - \alpha T^2 / (\beta + T) \quad (3)$$

we get $E_{g0} = 1.91$ eV, $\alpha = 4.4 \times 10^{-4}$ eV/K and $\beta = 93$ K. The value obtained for α , the temperature coefficient of the band gap, is low compared to that of $\text{Ga}_x\text{In}_{1-x}\text{P}$ alloys ($\approx 8 \times 10^{-4}$ eV/K). In general the value of α depends on the average phonon energy and the carrier-phonon coupling strength both of which are modified in a superlattice in comparison to the bulk solid,¹⁴ which may be the reason for its low value in our sample. However what is clear from the above study is that there is no apparent anomalous dip in the temperature dependence of the critical point energies in the sample.

B. Spectroscopic indications of QD formation

First of all we note that the broad 8 K PL feature A1 (at A) is typical of luminescence from QDs with finite size/composition distribution. In the present case the full width at half maximum (FWHM) of the PL feature A1 is ≈ 100 meV. This is larger than those reported for other self-organized alloy based QDs such as InAlAs/GaAs QDs (PL linewidth ≈ 60 meV at 77 K) which have been used to fabricate lasers.³ This is consistent with the fact that our measured size distribution¹⁰ ($\approx 25\%$) is larger than those of the InAlAs/GaAs QDs mentioned above ($\approx 15\%$). Thus there is scope for improvement in optimizing the growth of our samples. A simple envelope function calculation with the above men-

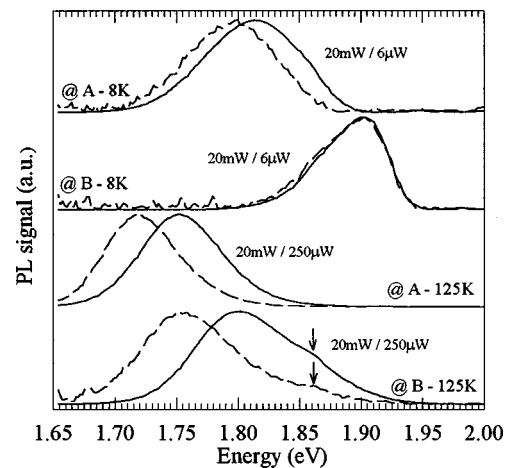


FIG. 5. Laser excitation power dependence of the PL spectrum at the two spots A and B at two different temperatures. The dashed lines represent the spectrum recorded with the lower excitation power. These spectra are normalized to get the same peak height. The laser spot diameter was ≈ 300 μm .

tioned QD size distribution and Ga concentration distribution $\Delta x \approx \pm 0.05$ (assumed uncorrelated to size distribution as a first approximation) does result in a PL linewidth of ≈ 100 meV.

Figure 5 shows the dependence of the PL peak position on the pump laser power. These spectra are normalized to get the same peak height. We find that at 8 K, the spectrum at A shows a blueshift with an increase in the excitation power while the spectrum at B (with feature B2 being dominant at 8 K) shows no measurable shift. However, when the temperature is raised to 125 K so that the feature B1 becomes dominant at spot B, we begin to observe similar pump power dependent shifts in the PL spectra at both the spots. Note that in the 125 K spectrum at B there exists a high energy shoulder (shown by arrow) whose position does not shift with change in excitation power. This shoulder is essentially a remnant of the feature B2 which shows no excitation power dependent peak shift. In these measurements the laser spot diameter was ≈ 300 μm , therefore the maximum excitation power density was ≈ 30 W/cm^2 . The blueshift of the PL spectrum even with such relatively low excitation power density is a characteristic property of luminescence from QDs.²³ The reason suggested for this is that in such samples the carriers generated in the regions surrounding the dots funnel into it. As a consequence, even for relatively small excitation power densities, phase space filling effects begin to show up prominently.²³ In fact, in cases where the QD size and composition has a narrow distribution it is possible to see new structures in the PL spectrum at higher energies, corresponding to carriers recombining from the higher lying states of the QDs as the excitation power is increased to ≈ 250 W/cm^2 (Refs. 24 and 25). Such accumulation of carriers in a small region is not expected in bulk or in 2D systems (in plane). Accordingly the feature B2, which we have already identified as arising from recombinations in the unmodified SPS phase, shows no measurable excitation power dependent peak position shift. The observation of pump power dependent blueshift of the PL spectra for features A1

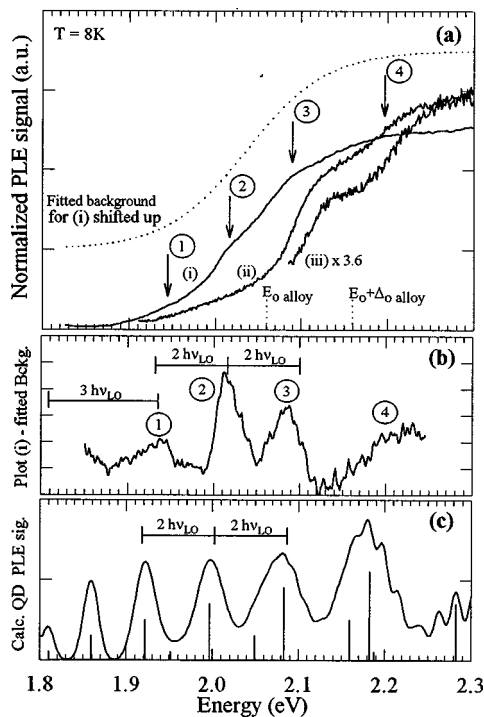


FIG. 6. (a) The photoluminescence excitation spectra of the sample at different detection energies (i) $E_d=1.81$ eV, at A, (ii) $E_d=1.9$ eV at B and (iii) $E_d=2.04$ eV at A. The dotted line is a smooth fitted background to the spectrum in plot (i) vertically shifted up for clarity. (b) The spectrum in plot (i) after background subtraction. (c) Simulated PLE spectra for the quantum dots including effects due to dot size, composition distribution and instrumental broadening. The vertical lines represent the ideal absorption spectra of a 210 Å diam dot.

and B1 is the first spectroscopic indication of QD formation in the SILCM modified layers of our sample. This results in the following additional source of error in estimating the temperature dependence of transition energies in QDs from PL measurements. For a given pump beam intensity, the excess carrier concentration in the QDs is temperature dependent. Therefore, phase space filling of the QDs is temperature dependent. Since the PL peak position in QDs depends strongly on the extent of phase space filling therefore the PL peak position does not provide an accurate measure of the variation of the critical point energies with temperature.

As a further investigation, we performed PLE experiments on this sample at different detection energies. The results are shown in Fig. 6(a). For the spectrum in plot (i) the detection energy $E_d=1.81$ eV corresponds to the peak position of the PL spectrum at spot A where we presume the luminescence arises predominantly from carrier recombinations in dots of size and composition (In concentration) that are most prevalent. In plot (ii) $E_d=1.9$ eV, which is close to the peak position of the PL spectrum at spot B where the luminescence arises from recombination in the SPS phase. In plot (iii) the spectrum was taken with $E_d=2.04$ eV at spot A (similar PLE spectrum is also obtained for this E_d at spot B), where the luminescence arises from recombination in the top $\text{Ga}_{0.57}\text{In}_{0.43}\text{P}$ layers. The two rising edges in plot (iii) represent the absorption at the E_0 and $E_0+\Delta_0$ gaps of $\text{Ga}_{0.57}\text{In}_{0.43}\text{P}$ alloys which are ≈ 98 meV apart. Plot (ii) has three rising features, the first one between 1.9 and 2.05 eV is

due to absorption in the SPS layers. The other two are identical to those seen in plot (iii) indicating that the carriers generated in the $\text{Ga}_{0.57}\text{In}_{0.43}\text{P}$ layers get transferred to the SPS layers which have lower band gap and finally recombine from there. However the spectrum in plot (i) is different. A closer inspection of this spectrum reveals four weak and broadened humps [indicated by the arrows in Fig. 6(a)], riding on top of a smoothly varying background. Although it is tempting to associate these humps in plot (i)_{PLE} with the features in the CER spectrum in Fig. 4, however a detailed comparison does not allow a one to one match between the features in the two sets of spectra. We suggest that all these weak humps in plot (i) arise due to absorption by the higher lying excited states of the QDs while the background has contributions from recombination of carriers that were originally generated in the $\text{Ga}_{0.57}\text{In}_{0.43}\text{P}$ layers and the SPS phase adjacent to the dots and then transferred to the QDs. We have made an attempt to bring out these weak resonant humps more clearly by subtracting from plot (i) a smooth background obtained by fitting to it the function $f(E)=a(1-1/\{\exp[(E-b)/c]+1\})$, where E is the energy and a, b, c are the fitting parameters. The fitted smooth background is shown by the dotted lines in Fig. 6(a) (vertically shifted for clarity) and the subtracted spectrum is shown in Fig. 6(b) where four peaks are clearly seen. It is well established that intradot exciton relaxation from higher excited states of a QD to the QD ground state is mediated by multiple phonon emission.^{24,25} As a result peaked structures are seen in the PLE spectrum of QDs whenever the excited and the ground state are separated by multiples of the longitudinal optical (LO) phonon energy ($h\nu_{\text{LO}}$)²⁶ and therefore separation between these peaks are also multiples of $h\nu_{\text{LO}}$. For an In rich $\text{Ga}_x\text{In}_{1-x}\text{P}$ alloy $h\nu_{\text{LO}}\approx 43$ meV and as seen in Fig. 6(b) the first three structures do have an average spacing of $2h\nu_{\text{LO}}$.

In order to make a preliminary estimate of the absorption spectrum of the QDs we performed a simple envelope function calculation where the QD was modeled by a spherically symmetric potential well of diameter 210 Å with infinite barriers. Only heavy hole absorption was considered (light hole absorption is smaller by more than a factor of 3) and carrier effective masses were obtained by appropriate linear interpolation between listed values²⁷ for InP and GaP. The other assumptions involve neglecting Coulomb effects and heavy hole–light hole mixing.²⁸ The former is strictly valid if the free exciton Bohr radius is much larger than the QD radius (in our case they are comparable) and the latter begins to influence the spectrum drastically²⁹ for heavy hole–light hole coupling constant ≈ 0.7 (in our case it is ≈ 0.5). In order to match the PL peak at 1.81 eV we had to consider a band gap of ≈ 1.763 eV for the In rich regions of the SILCM modified phase. The Ga concentration required to get this value for the band gap of a relaxed random $\text{Ga}_x\text{In}_{1-x}\text{P}$ alloy is $x=0.35$. This value of x (which might change somewhat when the appropriate strain tensor, as required in the present case, is taken into account) is close to the expected $\approx 0.4/0.6$ Ga composition contrast between the Ga deficient and Ga rich regions in the SILCM modified phase.^{8,30} The sharp vertical lines in Fig. 6(c) show the absorption spectrum for a 210 Å dot using the above model.

The continuous curve represents a simulated PLE spectrum (of only the dots) taking into account broadening due to dot size distribution, composition distribution ($\Delta x \approx \pm 0.05$ about mean Ga concentration x assumed), finite spectral width of the excitation source and the spectral band pass of the detection system. Multiple phonon emission related PLE signal enhancement was not considered in the above simulation. The above calculation makes many simplifying assumptions and so it is not surprising that the features in the simulated PLE spectra do not exactly match the features in Fig. 6(b). Nevertheless the simulated spectrum brings out the following two points in support of our suggestion: (i) the average spacings of some of the prominent calculated QD transitions are close to $2h\nu_{LO}$ and approximately match those of the features seen in Fig. 6(b), (ii) it shows that in spite of the large QD size and composition variation it is still possible to see resonant peaks in the PLE spectrum associated with QD transitions. The latter is because unlike CER or absorption measurements which are broadened by the total QD size and composition distribution to the extent that no QD related features can be resolved, in PLE one is able to selectively probe a narrow range within this distribution. This selectivity of PLE (and also resonantly excited PL) has in fact previously been exploited in the study of self-organized InGaAs/GaAs QDs.³¹

IV. CONCLUSION

In summary, we have reported results of the detailed spectroscopic study of Ga–In–P based self-organized QD like structures formed during the growth of $(\text{GaP})_2(\text{InP})_{2.5}$ SPS short period superlattices sandwiched between $\text{Ga}_x\text{In}_{1-x}\text{P}$ alloy layers on GaAs (311)A substrates. We have identified the origins of the various features in different spectra. Our results indicate the simultaneous presence of two major optically active phases in these samples. One is the original $(\text{GaP})_2(\text{InP})_{2.5}$ SPS layer while the other is the SILCM modified regions in some parts of the $(\text{GaP})_2(\text{InP})_{2.5}$ layer. This suggests that the SILCM modification of the SPS layers is incomplete. The SILCM modified In rich regions were shown to have a QD-like nature. The anomalous temperature dependence of the PL peak positions in such samples arises due to competition between two luminescence pathways: one associated with the QDs and the other with the original SPS layer phase. The photoluminescence quenching pathway for the QDs has also been determined.

ACKNOWLEDGMENTS

The authors thank Professor K. L. Narsimhan, Professor K. S. Chandrasekharan and T. K. Sharma for many useful discussions.

- ¹H. Asahi, *Adv. Mater.* **9**, 1019 (1997).
- ²N. N. Ledentsov *et al.*, *Phys. Rev. B* **54**, 8743 (1996).
- ³S. Fafard, K. Hinzer, S. Raymond, M. Dion, J. McCaffrey, Y. Feng, and S. Charbonneau, *Science* **274**, 1350 (1996).
- ⁴K. C. Hsieh, J. N. Baillargeon, and K. Y. Cheng, *Appl. Phys. Lett.* **57**, 2244 (1990).
- ⁵J. M. Millunchick, R. D. Twesten, S. R. Lee, D. M. Follstaedt, E. D. Jones, S. P. Ahrenkiel, Y. Zhang, H. M. Cheong, and A. Mascarenhas, *MRS Bull.* **22**, 38 (1997).
- ⁶S. Ghosh, B. M. Arora, S. J. Kim, and H. Asahi, *Superlattices Microstruct.* **24**, 127 (1998).
- ⁷K. Y. Cheng, K. C. Hsieh, and J. N. Baillargeon, *Appl. Phys. Lett.* **60**, 2892 (1992).
- ⁸P. J. Pearah, A. C. Chen, A. M. Moy, K.-C. Hsieh, and K.-Y. Cheng, *IEEE J. Quantum Electron.* **30**, 608 (1994).
- ⁹S. J. Kim, H. Asahi, M. Takemoto, K. Asami, M. Takeuchi, and S. Gonda, *Jpn. J. Appl. Phys., Part 1* **35**, 4425 (1996).
- ¹⁰J. H. Noh, H. Asahi, S.-J. Kim, and S.-I. Gonda, *Jpn. J. Appl. Phys., Part 1* **36**, 3818 (1997).
- ¹¹M. Kondow, S. Minagawa, Y. Inoue, T. Nishino, and Y. Hamakawa, *Appl. Phys. Lett.* **54**, 1760 (1989).
- ¹²B. T. McDermott, K. G. Reid, N. A. El-Masry, S. M. Bedair, W. M. Duncan, X. Yin, and F. H. Pollak, *Appl. Phys. Lett.* **56**, 1172 (1990).
- ¹³D. E. Wohlert, S. T. Chou, A. C. Chen, K. Y. Cheng, and K. C. Hsieh, *Appl. Phys. Lett.* **68**, 2386 (1996).
- ¹⁴F. H. Pollak and H. Shen, *Mater. Sci. Eng., R.* **10**, 275 (1993).
- ¹⁵X. Yin and F. H. Pollak, *Appl. Phys. Lett.* **59**, 2305 (1991).
- ¹⁶S. Ghosh and B. M. Arora, in *Proceedings of International Conference on Instrumentation*, edited by B. S. Ramprasad, S. Asokan, K. Rajanna, and N. C. Shivaprakash (New Age, Bangalore, 1996).
- ¹⁷H. Nashiki, I. Suemune, H. Suzuki, and K. Uesugi, *Jpn. J. Appl. Phys., Part 1* **36**, 4199 (1997).
- ¹⁸G. Armelles, M. C. Munoz, and M. I. Alonso, *Phys. Rev. B* **47**, 16299 (1993).
- ¹⁹L. Aaigouy, T. Holden, F. H. Pollak, N. N. Ledentsov, V. M. Ustinov, P. S. Kop'ev, and D. Bimberg, *Appl. Phys. Lett.* **70**, 3329 (1997).
- ²⁰S. Weber, W. Limmer, T. Thinke, R. Sauer, K. Panzlaff, G. Bacher, H. P. Meier, and P. Roentgen, *Phys. Rev. B* **52**, 14 739 (1995).
- ²¹S. Fafard, S. Raymond, G. Wang, R. Leon, D. Leonard, S. Charbonneau, J. L. Merz, P. M. Petroff, and J. E. Bowers, *Surf. Sci.* **361**, 778 (1996).
- ²²Y. P. Varshini, *Physica (Utrecht)* **34**, 149 (1967).
- ²³L. Samuelson *et al.*, *Jpn. J. Appl. Phys., Part 1* **34**, 4392 (1995).
- ²⁴S. Fafard, R. Leon, D. Leonard, J. L. Merz, and P. M. Petroff, *Phys. Rev. B* **52**, 5752 (1995).
- ²⁵N. N. Ledentsov *et al.*, *Solid-State Electron.* **40**, 785 (1998).
- ²⁶K. H. Schmidt, G. Medeiros-Ribeiro, M. Oestreich, P. M. Petroff, and D. H. Dohler, *Phys. Rev. B* **54**, 11 346 (1996).
- ²⁷*Landolt-Bornstein Numerical Data and Functional Relationships in Science and Technology*, edited by O. Madelung, W. von der Osten, and U. Rossler, New Series Vol. III/22a (Springer, Berlin, 1987).
- ²⁸U. Woggon, *Optical Properties of Semiconductor Quantum Dots* (Springer, Berlin, 1997).
- ²⁹L. Banyai and S. W. Koch, *Semiconductor Quantum Dots* (World Scientific, Singapore, 1993).
- ³⁰P. Dua, S. L. Cooper, and K. Y. Cheng, *Appl. Phys. Lett.* **72**, 1072 (1998).
- ³¹S. Fafard, D. Leonard, J. L. Merz, and P. M. Petroff, *Appl. Phys. Lett.* **65**, 1388 (1994).